PERIODIC VARIATION OF δ ^{18}O VALUES FROM V28-239 PACIFIC OCEAN DEEP-SEA CORE

J. XANTHAKIS[1],* I. LIRITZIS[1] and A. TZANIS[2]
[1]*Research Center for Astronomy and Applied Mathematics, Academy of Athens, 14 Anagnostopoulou str., Athens 106 73, Greece;* [2]*Department of Geology, Geophysics-Geothermy Division, University of Athens, Greece*

(Received 9 June 1994)

Abstract. Spectral analysis of δ^{18}O values from V28-239 pacific ocean deep-sea core has revealed periodicities which correspond to those calculated for the eccentricity (400 and 100 Kyrs), the obliquity (41 Kyrs) and the climatic precession (23 and 19 Kyrs) as well as secondary ones spanning between 16 Kyrs to 1 million years. The methods of spectrum analysis applied were the maximum entropy, fourier and the successive approximations, where the periodicities are located and their amplitude defined.

The significance and stationarity of the detected periods was examined by various tests as well as employing an evolutionary pseudosonogram.

The dominant 100 Kyrs and 50 Kyrs periods are present throughout all the interval, the 30 Kyrs is at low variance during 1.2 to 2 million years interval, the precessional signal is not stationary and appears at about 600 Kyrs to 1820 Kyrs.

This study shows the necessity of applying various spectral analysis techniques and several tests to extract the optimum of spectral information and also to test the stationarity of certain periodicities, especially when implied mechanisms of climatic cause and variability are involved.

Introduction

Among the longest astrophysical and astronomical cycles that might influence climate, and even among all forcing mechanisms external to the climatic system itself, only those involving variations in the elements of the earth's orbit have been found to be significantly related to the long-term climatic data deduced from the geological record.

A fundamental tool for the palaeoclimatic interpretation of geological records involves the Oxygen-18 stable isotope technique that has been an invaluable aid in examining the climatic history of the past million years.

The most commonly used fossils for O-18 analyses are foraminiferas, single-celled amoeba-like organisms with $CaCO_3$ shells. There are both planktonic (surface and near surface) and benthic (bottom dwelling) varieties.

The fundamental geological problem associated with O-18 interpretations involves the realization by Emiliani (1955) that the environmentally temperature dependant ^{18}O content of seawater can also be affected by the formation of ice sheets.

* Deceased.

Earth, Moon and Planets **66:** 253–278, 1995.

Analyses of $^{18}O/^{16}O$ time-series adds to the international effort which is to explain the astronomical theory of palaeoclimates that provides us with the opportunity to better understand the dynamical behavior of the climatic system.

In the last twenty years the astronomical theory of climate forcing gained much respect. According to this theory of palaeoclimates – a particular version of which is referred to as the Milankovich theory – the long-term variations in the geometry of the earth's orbit and rotation are the fundamental causes of comings and goings of Pleistocene ice-ages of the past 2 or 3 million years.

This Milankovich theory is strongly supported from spectral analysis of various deep-sea sediment core records which show periodicities corresponding to those calculated in the astronomical record of eccentricity (400 and 100 Kyrs, 1 Kyr = 1,000 years), axial tilt or obliquity of 41 Kyrs and precession (19 and 23 Kyrs).

It was Hays *et al.* (1976) who demonstrated that the astronomical frequencies were significantly present in palaeoclimatic data; the 100-, 41-, 23-, and 19-Kyrs periods are superimposed on a general red noise spectrum.

Since then, the Milankovich renaissance emerged from spectral analysis of proxy climatic data (coral reefs, Caribbean, Indian, Pacific and Atlantic deep-sea cores), detailed astronomical data from celestial mechanics and climatological models (Berger, 1988).

However, within the present stage of our knowledge, other factors controlling the climate but evolving at a much slower rate (such as the geographical distribution of the continents and the solar luminosity) must be assigned values appropriate for the beginning of the Pleistocene.

Although evidence that the astronomical frequencies are also found in the remote geological past has accumulated (Berger, 1989), it is not known whether the astronomical mechanism continues to play a fundamental role in modulating the climate of a different geographical world (controlled by plate tectonics) or of a differently insulated planet (variations in the total energy input to the earth being controlled by the sun, the interstellar matter or the atmospheric composition).

The aim of the present work is:

(a) to spectrally analyse the Oxygen-18 per mil values of planktonic foraminifera from the Pacific ocean deep-sea core V28-239 spanning the past 2 million years, in sampling intervals of 5 Kyrs. A single analysis, comprising of 15 specimens of *Globigerinoids sacculifer*, has been made at each level in the core. The uncertainty in analysis of a single sample from the sediment combining isotopic variability and analytical precision is $\pm 0.11‰$.

The data set was taken from the paper by Shackleton and Opdyke (1976). These values vary between $-0.5‰$ and $-1.7‰$, which with use of the temperature versus $\delta^{18}O$ per mil empirical equation of Emiliani (1955), correspond to summer insolation temperature values of 22.5° to 28.5° respectively. This is an approximate estimation and infers sea surface temperature without taking care of ice volume changes, albeit in the pacific a different situation prevails, the O-18 isotope com-

position of *G. sacculifer* corresponds to a temperature several degrees below sea surface similar to isotopic records of benthic species in core e.g V28-238.

(b) To investigate the linear behaviour of pleistocene climate response and its variability at astronomical frequencies.

The methods employed are: MESA, Periodogram (Fast Fourier Transform, FFT), Blackman-Tukey smoothed spectrum analysis (PSA) attaching significance levels and fitting the data with Successive Approximations method (SA). Tests of significance (i.e. the Kolmogorov–Smirnov test) and stationarity (Pseudosonogram, use of various autoregressive, AR, orders) were applied (Xanthakis and Liritzis, 1991).

First the MESA and FOURIER and PSA methods were applied in order to identify any hidden periodicities (Chatfield, 1984), followed by the newly used SA method, where the identified periods were actually defined in the time-series, their amplitude determined and their stationarity easily assessed.

Spectrum Analysis Methods

A) Maximum Entropy (MESA) and FFT

The MESA method of Ulrych and Bishop (1975) is based on algorithms developed by Burg (1967, 1968), Anderson (1974) and Smylie *et al.* (1973) (see Barton, 1983).

In this analysis use was made of the Akaike's final prediction error (FPE) criterion. Figure 1 (Akaike, 1969).

The raw data were first smoothed by subtraction of their mean value.

This criterion exhibits the expected, monotonically decreasing character as a function of the order of AR filter, to the length of $M = 58$. For $M > 60$ its behaviour changes to a monotonically increasing one, with low gradient. This kind of behaviour is believed to be a result of data overfitting. As will be seen shortly, $M = 60$, which corresponds to a time interval of 300 Kyrs, is approximately, the time interval of the longest significant period in the data, that is shorter than the fundamental. At this point most of the structured information is extracted from the data; beyond this point the MESA processor will attempt to fit exactly the high frequency spectral contributions as well as noise. As will be seen however, there exists a power differential of two orders of magnitude between high and low frequency contributions in our data: the exact fitting of wide-band data with such a variation in power content is not an easy task to accomplish.

The most probable result will be the introduction of spurious singularities in the resulting wavelet frequency variance (residual error power) and spurious spectral lines. The effect will progressively expand from higher to lower frequencies and will influence the FPE function. We can demonstrate the above assessments with comparisons of MESA power spectra for different lengths M of the AR process, as well as with direct comparisons of MESA and FFT power spectra.

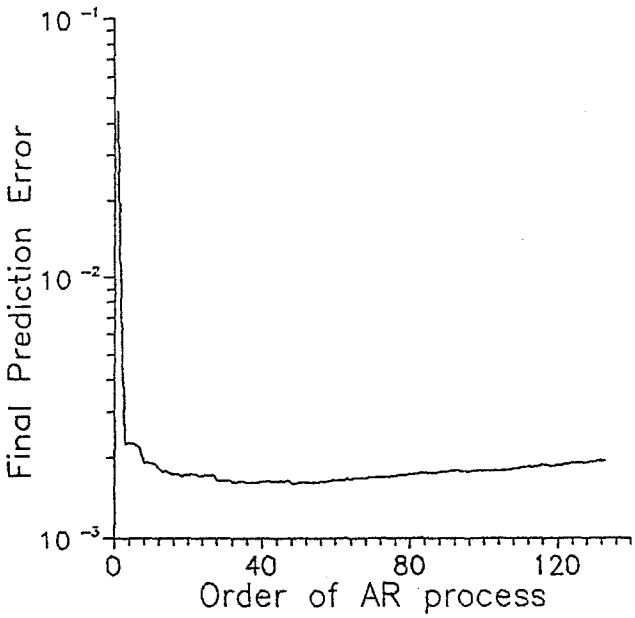

Fig. 1. Akaike's final prediction error (FPE) as a function of the AR order.

In Figure 2a the normalized MESA power spectrum of our time-series computed for an AR order of $M = 60$, is shown.

In Figure 2b the normalized MESA power spectrum computed for an AR order $M = 100$ is presented.

When Figures 2a and 2b are compared, we can see that almost all the spectral peaks resolved by the $M = 60$ AR process can still be detected with the $M = 100$ AR process, except that additional spectral peaks have been introduced and the variance of the spectrum density function (SDF) increased appreciably, especially in the shortest period band (10–60 Kyrs). The variance of the SDF will certainly increase, as the order M increases. Some of the additional peaks may be spurious, others may correspond to physical processes. With the information available in the data we have no means of telling; such conclusive inferences can only be made if theoretical predictions are used for control.

Two additional powerful spectral peaks can be found in Figure 2b, in the vicinity of $T \sim 340$ Kyrs with an amplitude of 11% of the maximum, and in the vicinity of $T \sim 145$ Kyrs, with an amplitude of 10% of the maximum. The first feature cannot be seen in Figure 2a, possibly because it is longer than the time interval spanned by the $M = 60$ AR process (and the 60th order of autocorrelation function). The second feature will be discussed in due course. Such effects define, in a sense, the degree of caution that must be exercised when analysing wide-band data with variable power content.

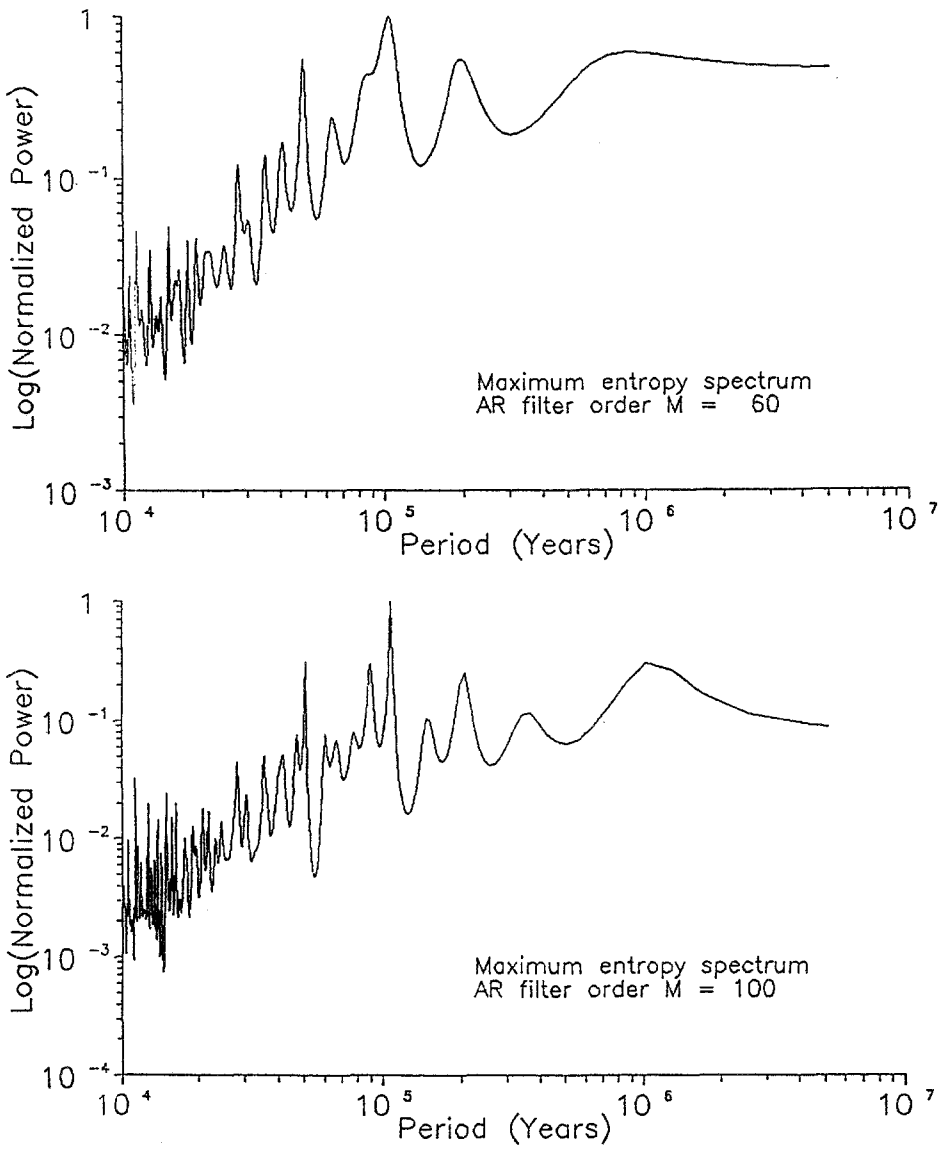

Fig. 2. (a) Log MESA spectrum of normalised power for AR filter order $M = 60$ and the periods in year. (b) Log MESA spectrum of normalised power for AR filter order $M = 100$ and the periods in years.

Because of the inconclusive performance of FPE, we consider it necessary to implement additional means of establishing the sufficient order of AR process. Such means can be the direct comparisons of MESA and FFT power spectra. For the sake of brevity and clarity, only a comparison of the $M = 60$ SDF (continuous line) and Blackman-windowed FFT SDF (dashed line), is presented in Figure 3;

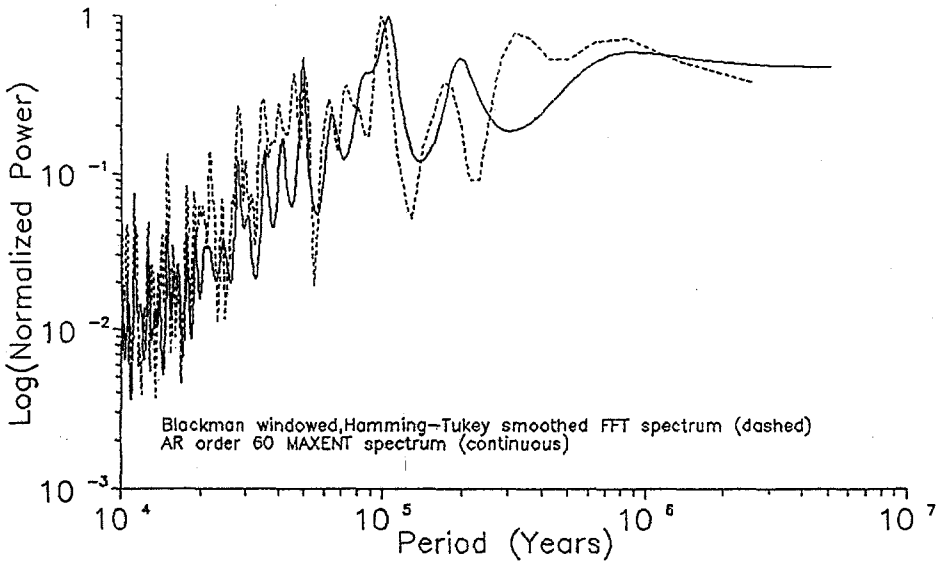

Fig. 3. Fourier (FFT) spectrum (dashed line) and MESA spectrum (solid line) of normalised power for $M = 60$ and periods in years.

the FFT SDF is presented after smoothing with a Hamming–Tukey window, to reduce the otherwise considerable variance of the short periods (dashed line).

Both SDFs are normalised to unity. The comparison indicates that, with the exception of $T \sim 340$ Kyrs spectral feature, all significant peaks in the MESA and FFT spectra compare one for one. The direct association of the spectral features detected by the two methods serves as clear indication that the M=60 processor has extracted most information available in the data, at least for the period band $T < 100$ Kyrs. In addition, the MESA SDF is more stable, exhibiting significantly less variance than all other SDFs, FFT or MESA with $M > 60$. The variance of the FFT and higher order MESA spectra can be reduced only by sacrificing resolution in the resulting SDF.

As a consequence of the above comparisons and the information provided by the FFT, the application of Occam's razor for our data would appear to indicate that an AR process of $M = 60$ is sufficient to describe most of the information available in the time-series; higher order AR processes will not necessarily extract more significant and interpretable information than we already acquired, at least for periods $T < 300$ Kyrs. It may be possible to process and extract more information by increasing M, but only at the expense of stability and smoothness in the SDF, with a consequent loss of resolution. The data at hand are wide-band and an AR process of order 60 will underfit spectral contributions with periods $T > 300$ Kyrs, so that a MESA spectral analysis with $M > 60$ is required in order to resolve them. Herein we use the SDF derived from an AR process with $M = 100$.

TABLE I

Summary of periodicities obtained by MESA, FOURIER and SA methods and comparison with fundamental and secondary periodic elements of earth's orbit, i.e., precession, obliquity and eccentricity.

Spectrum analaysis: periods for core V28-239 $\delta^{18}O$‰ (in Kyrs)					
			Astronomical elements		
MESA	FFT	Succes. apr.	Eccentr.	Precess.	Obliq.
1000	1000	1000	(1300)		
	500		(600)		
340			413		
	250				
200	200	180			
145	145	140			
100	105	100	95–136		
89	85	90			
		80			
64	67	60			
50	45–50	50			41
41		40		(56)	(53)
35	35				(30)
30	29.5	30			
27.6	20.8	20		19–23	
17.5	18				
16.2	16.2			(17)	
14.8	15.6	15		(15)	
12.5					
11.2		( ): Secondary peaks			

Based on the analysis detailed above, we have compiled Table I, which summarizes the significant spectral features (periodicities) detected in our data.

The next step in our analysis, was to conduct a study of possible evolutionarity in the data series at hand, i.e., a study for possible time variation of the spectral content in the analysed time-series (alternatively test its stationarity). From the data analysis point of view, such an exercise will provide additional means for testing and confirming the reliability and validity of the conclusions summarized in Table I, inasmuch as the MESA theory applies only to stationary processes and the method should be used in this capacity. From a physical point of view, this exercise will indicate the existence of non-stationary (time variable) processes registered in the palaeoclimatic history told by the analysed data.

The pseudo-sonogram of Figure 4 was constructed using a pseudo-ensemble approach. Thus, the original data series of 2,095 Kyrs duration (419 points) was

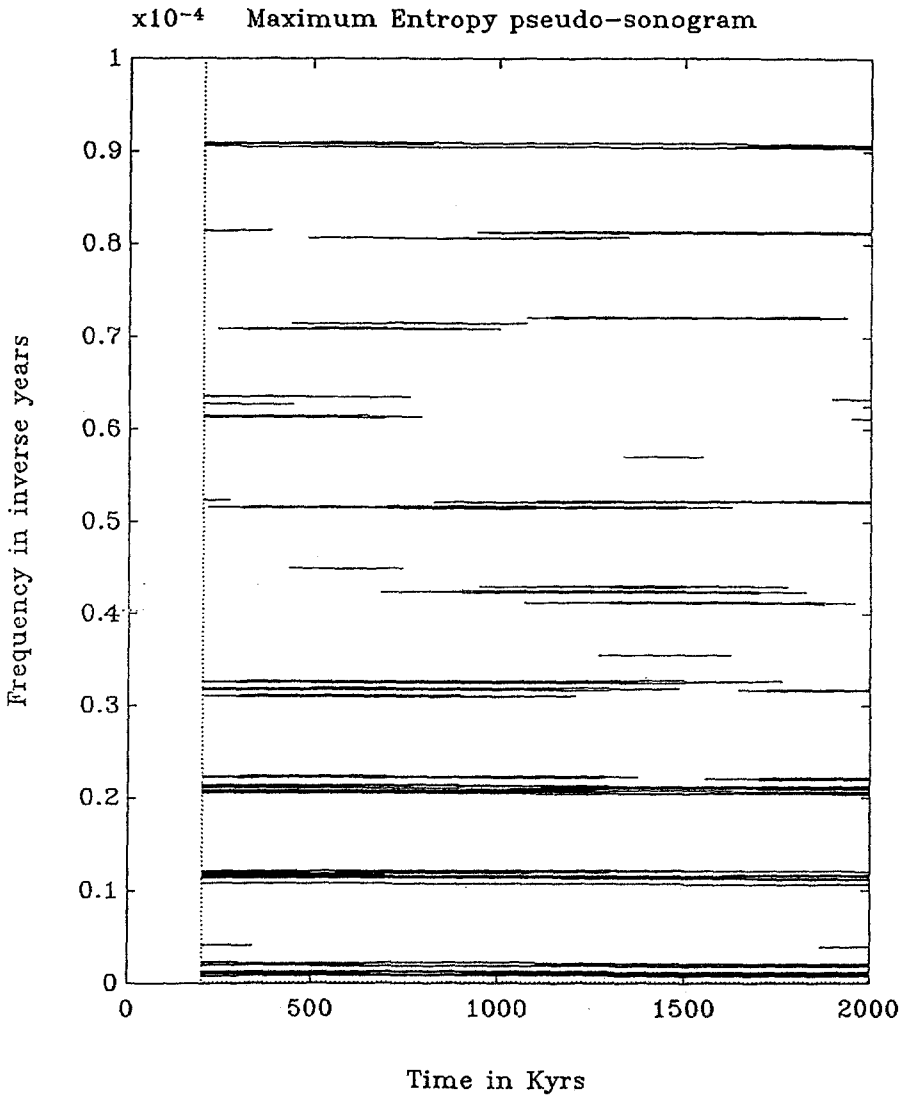

Fig. 4. Maximum entropy pseudosonogram showing the evolutionary temporal variation of periods. Ordinate scale is in frequency = periods^{-1}, and abscissa indicates the interval occupied by the time-series.

divided in 10 segments of 200 Kyrs duration (each 40 points long) and subjected to MESA spectral analysis. In order to choose the best AR order, the FPE criteria for each segment separately were compared. It turned out that an AR order length between 20–25 would satisfy the FPE criteria also. Therefore, an average AR order of $M = 23$ was chosen, which lies also within the Berryman ($M = 2N/\ln 2N$, N = no. of data) and Ulrych–Bishop upper limit ($M = N/2$) criteria.

The power spectra of each segment were then collated and contoured to produce Figure 4; a variable contour interval was chosen which, in combination with the high frequency resolution of the MESA method, resulted in the banded appearance of the sonogram. The dark bands correspond to continuous (stationary) powerful spectra peaks.

Of these, the band at the low frequency end of the spectrum (bottom end of Figure 4) corresponds to residual power in the long period end of the segmented data. Because the long period ($T > 200$ Kyrs) content of each segment could only be seen as a superposition of truncated sinusoids, it is doubtful whether the MESA method extracted valid spectral features or only artificial approximations of the long period trends in the data segments. The two closely spaced bands correspond to spectral peaks centered at about 850 Kyrs and 425 Kyrs. Their relationship rather supports the notion of artificiality of these features (the former is twice the period of the latter).

The remaining dominant spectral features detected in the previous analysis can be seen in Figure 4.

The two bands at approximately 0.1×10^{-4} yr^{-1} and 0.2×10^{-4} yr^{-1} correspond to the 100 Kyrs and 50 Kyrs spectral peaks detected above, and their associated side structure. The series of closely spaced bands just above the tick mark of 0.3×10^{-4} yr^{-1} can be attributed to the circa 30 Kyrs period. Other continuous or quasi-continuous bands correspond to the circa 18 Kyrs period (just above the tick mark of 0.5×10^{-4} yr^{-1}), the 15 Kyrs period (just above the tick mark of 0.7×10^{-4} yr^{-1}), the 12.5 Kyrs period (just above the tick mark of 0.8×10^{-4} yr^{-1}) and the 11 Kyrs period (just above the tick mark of 0.9×10^{-4} yr^{-1}). A series of bands circa the 25 Kyrs (around the tick mark of 0.4×10^{-4} yr^{-1}) appears between 600 and 1,800 Kyrs ago.

These results indicate the stationarity of the dominant spectral features in the data at hand, thus confirming of the validity and reliability of the MESA results derived from the original data series; this also appear to suggest the time invariance of the physical processes that generated the data i.e. the stationarity of the climatic processes registered in the data.

The data set is subsequently analysed with periodograms of FFT and PSA.

B) Periodogram (FFT) and power spectrum analysis (PSA)

Initially the time series was smoothed with a 5-point (=25 Kyrs) running mean, (abbreviated to O(5)18) and subsequently a sinusoidal fit of 1 million years period was subtracted from the smoothed values. The FFT power spectrum of the residual data set is shown in Figure 5a while Figure 6 gives the respective Kolmogorov–Smirnov test with the significance bands at 75% and 90% confidence levels.

The obtained periods are: 15.6, 16.2, 17–18, 21, ~25, 29.5, 35 and 50 Kyrs.

The smoothed Oxygen-18 values (O(5)18) were detrended also with a 1st order polynomial and subsequently analysed. Figure 7a.

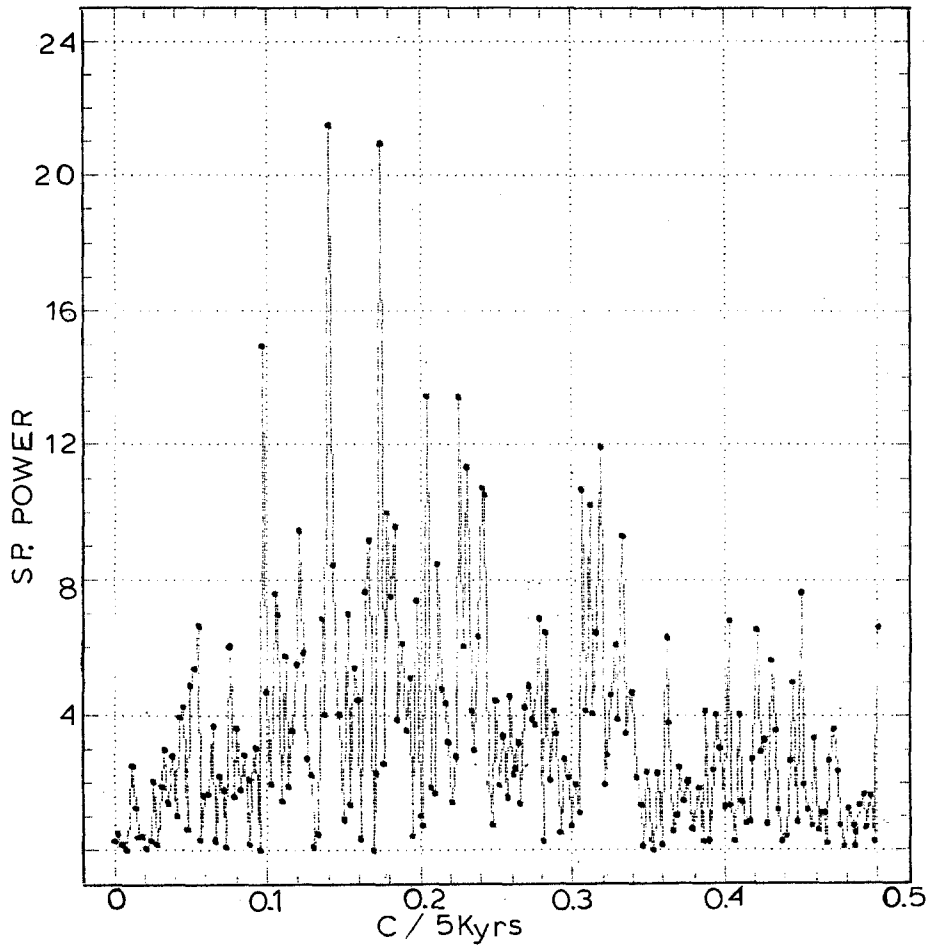

Fig. 5. Fourier spectrum (FFT) as a function of frequency in cycles per 5 Kyrs of the residual $\delta^{18}O$ data (=smoothed data with 5 points or 25 Kyrs, running mean, minus a sinusoidal fit with period of 1 million years).

The obtained periods were; 36, 45–50, 67, 85, 100, 145, 200–250, 500 Kyrs and 1 million years, with significance >90%.

Power (variance) spectra of the two above detrended time series (of Figure 5 and Figure 7) were obtained using the Blackman–Tukey approach.

The spectra were obtained from autocorrelation functions which were truncated either at 30 lags for subsets of 1/4th of total record or at 60–250 lags for the whole time series.

The ratio of the peak to the underlying continuum in the vicinity of the peak is used to test significance, then a Chi-square test shows if the ratios are significant at 1, 5 and 10% level (Silverman and Shapiro, 1983; Silverman *et al.*, 1971).

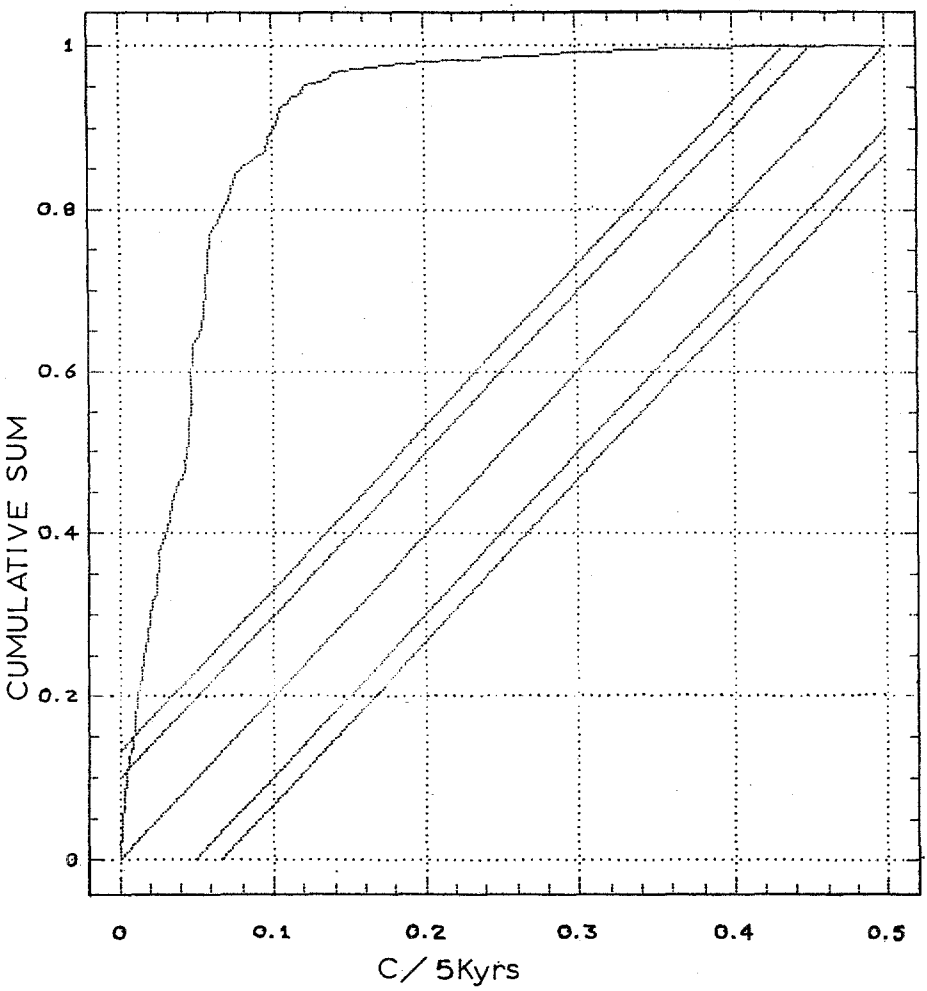

Fig. 6. Integrated periodogram (Kolmogorov–Smirnov test) indicating significance of periods. The two bands correspond to 75% (inner) and 90% (outer) significance.

The periodicities detected by the PSA and the attached significance levels are as follows: 1 million years (91%), 500 ± 80 Kyrs (89%), 200 Kyrs (>99%), 135 ± 20 Kyrs (97%), 100 ± 5 Kyrs (98%), 70 ± 5 Kyrs (99%), 50 ± 3 Kyrs (94%), 35 ± 2 Kyrs (85%). The lower than 35 Kyrs periods were of very low resolution and their underlying continuum (noise) confined their significance to 70–75%.

c) Successive approximations (SA)

The method has been described elsewhere (Xanthakis and Liritzis, 1991, 1989; Xanthakis *et al.*, 1992). First the raw data set is smoothed by running means and the mean value or the trend of the smoothed time series is subtracted. The obtained

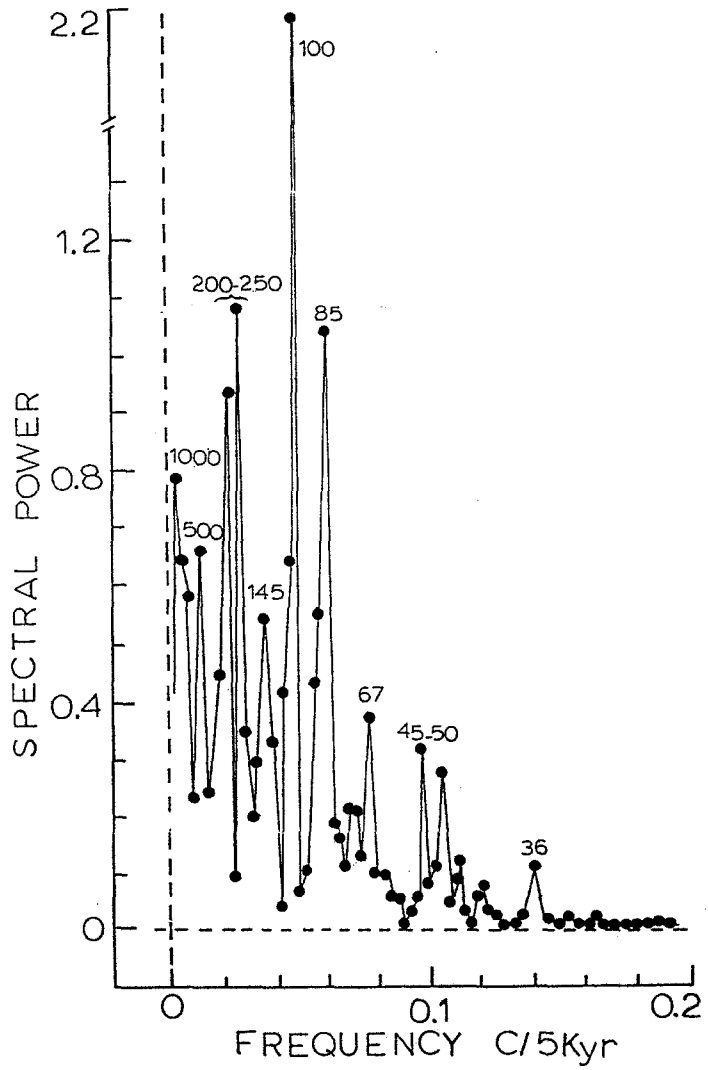

Fig. 7. Fourier spectrum (FFT) as a function of frequency in cycles per 5 Kyrs of the residual $\delta^{18}O$ data (=smoothed data with 5-points or 25 Kyrs running mean, minus a 1st order polynomial.)

differences are graphically examined by fitting the series with trigonometric series (least squares), with the end result being the representation of the time-series with an analytical expression. In this way the amplitude and position of the obtained periodicities are defined. The criteria used to choose the detected periodicities, in this way, which are located and described on the actual time series record, are in fact based upon the priorly obtained periodicities by the standard methods of spectrum analysis.

TABLE II

α_{1-9} coefficients of periodic terms of Equation (2) and respective time intervals (multiply with 5 Kyrs) where the periods appear

a_1	T
−0.30	423–417
0.08	420–417, 374–371, 232–226, 113–110
0.10	329–326, 20–17
−0.08	256–252
0.15	176–173
−0.15	172–169
−0.10	159–156
0.20	107–104
−0.25	35–32

a_2	T
−0.08	241–237
−0.25	44–40
0.15	12–8

a_3	T
−0.20	223–213
−0.15	201–191
0.10	155–150
−0.20	57–52

a_4	T
−0.10	390–384, 339–327, 278–272
0.10	320–308, 273–267, 236–230
−0.15	306–300, 151–145
0.15	293–287, 248–242, 180–174, 98–92, 63–57
−0.20	213–201, 17–11
−0.25	160–154, 119–113
0.30	75–63, 24–18
0.20	45–33
0.45	4–(−2)

a_5	T
−0.20	165–157
0.40	133–125
0.50	113–105
−0.40	13–4

TABLE II
Continued

a_6	T
0.20	361–352
−0.30	350–332
−0.25	287–278
0.25	193–184
−0.40	13–4

a_7	T
0.15	417–407
0.30	383–373, 95–85
0.20	327–317
−0.40	175–165, 55–45
−0.30	123–113, 84–74
0.50	107–97
−0.20	373–363
−0.70	34–24

a_8	T
0.25	261–247

a_9	T
−0.30	406–388

This approach first presented by Xanthakis and Liritzis (1986), offers six advantages; (i) locates the periods in the time series, (ii) measures their amplitudes, (iii) locates change of phase, (iv) infers of any combined effect of several periods (network of periodicities), (v) it exhibits a stepwise control of the analysis and (vi) provides an analytical expression of the phenomenon.

Due to (iv) above the obtained dominant periodicities by the standard methods of spectrum analysis may not be apparently seen as stationary in the original time series, but as quasi-periods or are overmasked by other periodicities.

The SA methodology involves a considerable amount of parameters, while such modelling of data is an attempt to describe a signal which is the superposition of several simple components, with prior subtraction of the trend.

Here the *mean trend* of the variation of the previously smoothed with a 5-terms running mean time-series is obtained, described by Equation (1):

$$\overline{\mathrm{O}(5)18} = -1.03 - 0.30 \sin(2\pi/10^6)(T - 825,000), \tag{1}$$

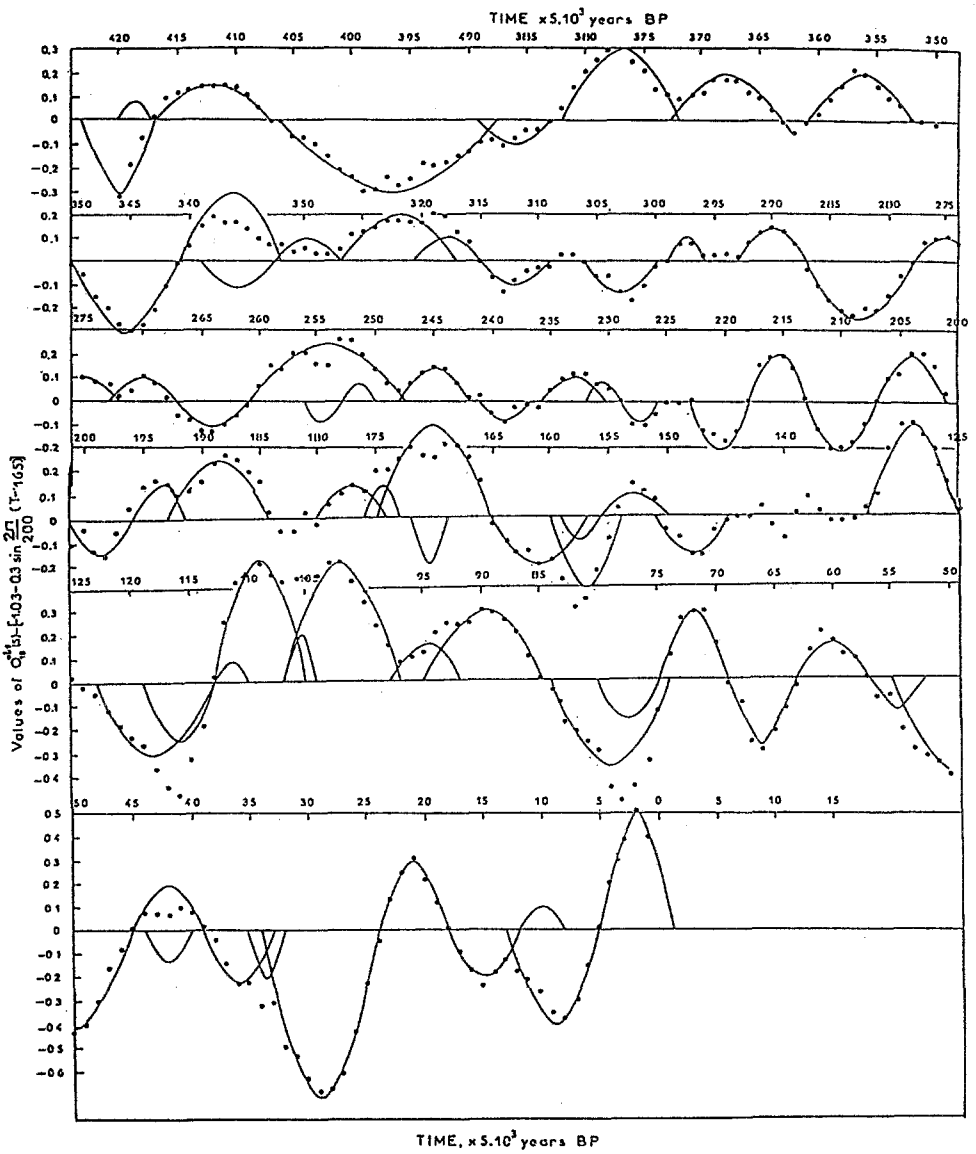

Fig. 8. Periodic variation (solid curve) described by successive approximations fit of the smoothed with 5-points δ^{18}O values (dots), minus the mean trend of $\overline{O18(5)} = -1.03 - 0.30 \sin 2\pi(T - 825000)/10^6$ (Equation (1) in the text). (Note that the numbers inside the parenthesis are multiplied by 5 Kyrs.)

(The one million sinusoidal periodic term starts from 825,000 years BP completes its half cycle in 325,000 years BP and ends at some distant point of 175,000 years after present, AP, see Figure 9.)

The differences between *smoothed values* and the *mean trend*, $W = \mathrm{O(5)18} - \overline{\mathrm{O(5)18}}$, exhibit (quasi-) periodic variations expressed by Equation (2):

$$\begin{aligned} P = {} & a_1 \sin(2\pi/30,000)T + a_2 \sin(2\pi/40,000)T + \\ & + a_3 \sin(2\pi/50,000)T + a_4 \sin(2\pi/60,000)T + \\ & + a_5 \sin(2\pi/80,000)T + a_6 \sin(2\pi/90,000)T + \\ & + a_7 \sin(2\pi/100,000)T + a_8 \sin(2\pi/140,000)T + \\ & + a_9 \sin(2\pi/180,000)T \end{aligned} \tag{2}$$

The periodicities detected here are; 30, 40, 50, 60, 80, 90, 100, 140 and 180 Kyrs.

Figure 8 shows these periods. Table II provides the a_1–a_9 coefficients. The a_{1-9} are the coefficients of periodic terms. Every coefficient has the numeric values of respective time intervals. The analytical expression which approximates O(5)18, i.e., the computed O(5)18 comp., is the sum of

$$\text{Eq. (1)} + \text{Eq. (2)} = \overline{\mathrm{O(5)18}} + P = \mathrm{O(5)18\ comp.} \tag{3}$$

and it is represented by the solid curve of Figure 8.

Figure 9 gives the *computed* and *smoothed* values of O(5)18. The analytical expression of Equation (3) approximates the smoothed values with an accuracy of 97.3%, a standard error of ± 0.028, it consists of 156 parameters (P) and has 264 degrees of freedom (DF).

(Note that the 156 parameters, P, is the sum of numeric values a_i plus the set of periods expressed by two numbers, which mark the beginning and the end of each period. This sum must be smaller than the number of data points in the figure, hence the degrees of freedom is positive, $DF > 0$, DF = No. of points $- P$).

Subsequently, the difference between the *initial unsmoothed* δ^{18}O values and the *computed smoothed* ones were analysed.

Figure 10 presents these differences as well as the periodic terms of 15, 20 and 30 Kyrs, which fit the difference.

The final generalized expression describing the *computed* oxygen values, by the SA method, of the original (raw) *unsmoothed* ones is given by Equation (4) and are depicted in Figure 11.

$$\mathrm{O(18)comp} = \mathrm{O(5)18comp} + P_1, \tag{4}$$

where

$$\begin{aligned} P_1 = {} & a_1 \sin(2\pi/15,000)T + a_2 \sin(2\pi/20,000)T + \\ & + a_3 \sin(2\pi/30,000)T. \end{aligned} \tag{5}$$

The coefficients a_{1-3} are given in Table III.

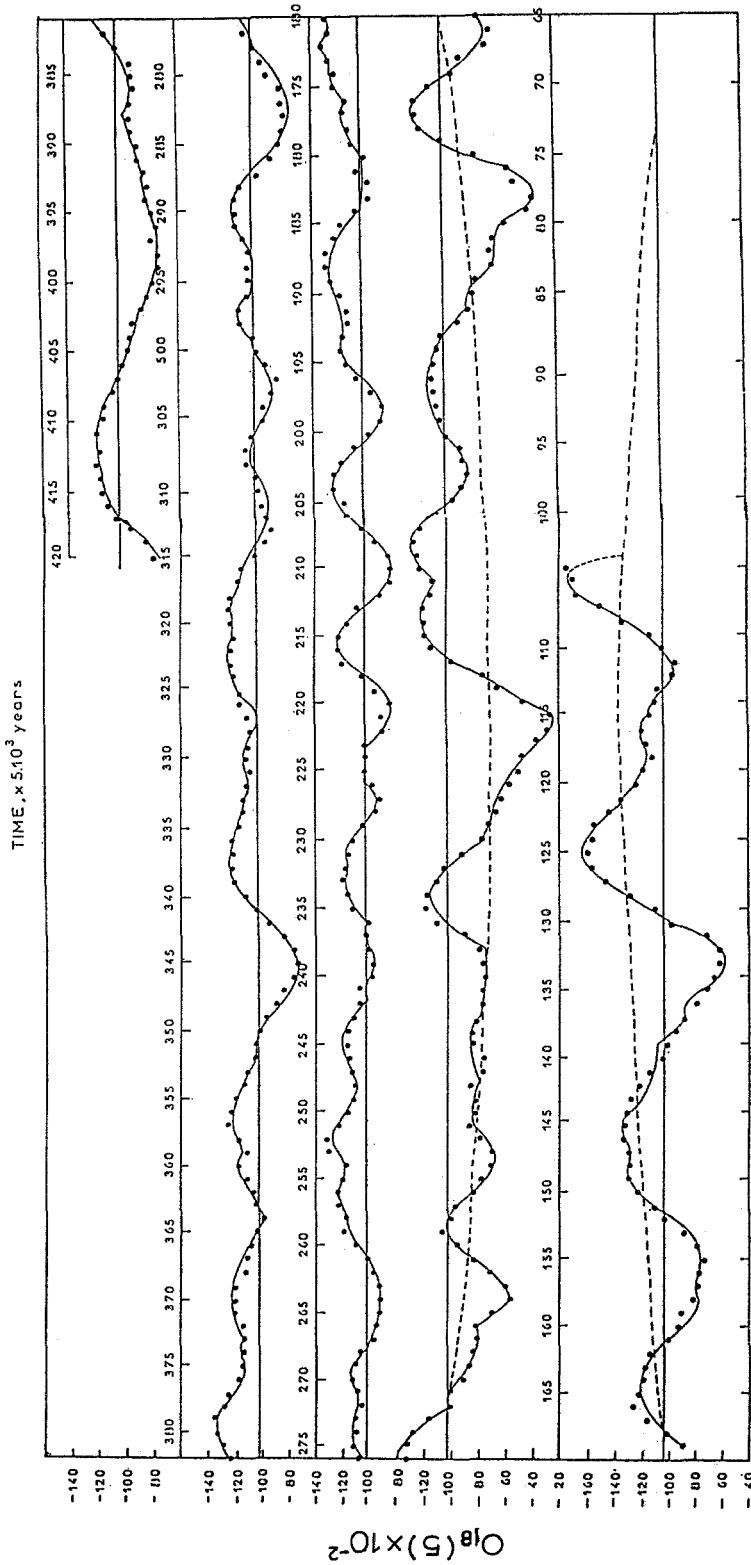

Fig. 9. Computed δO(5)18 comp. values (solid) by Equation (3) in the text and smoothed δO(5)18 values (dots), with the SA method.

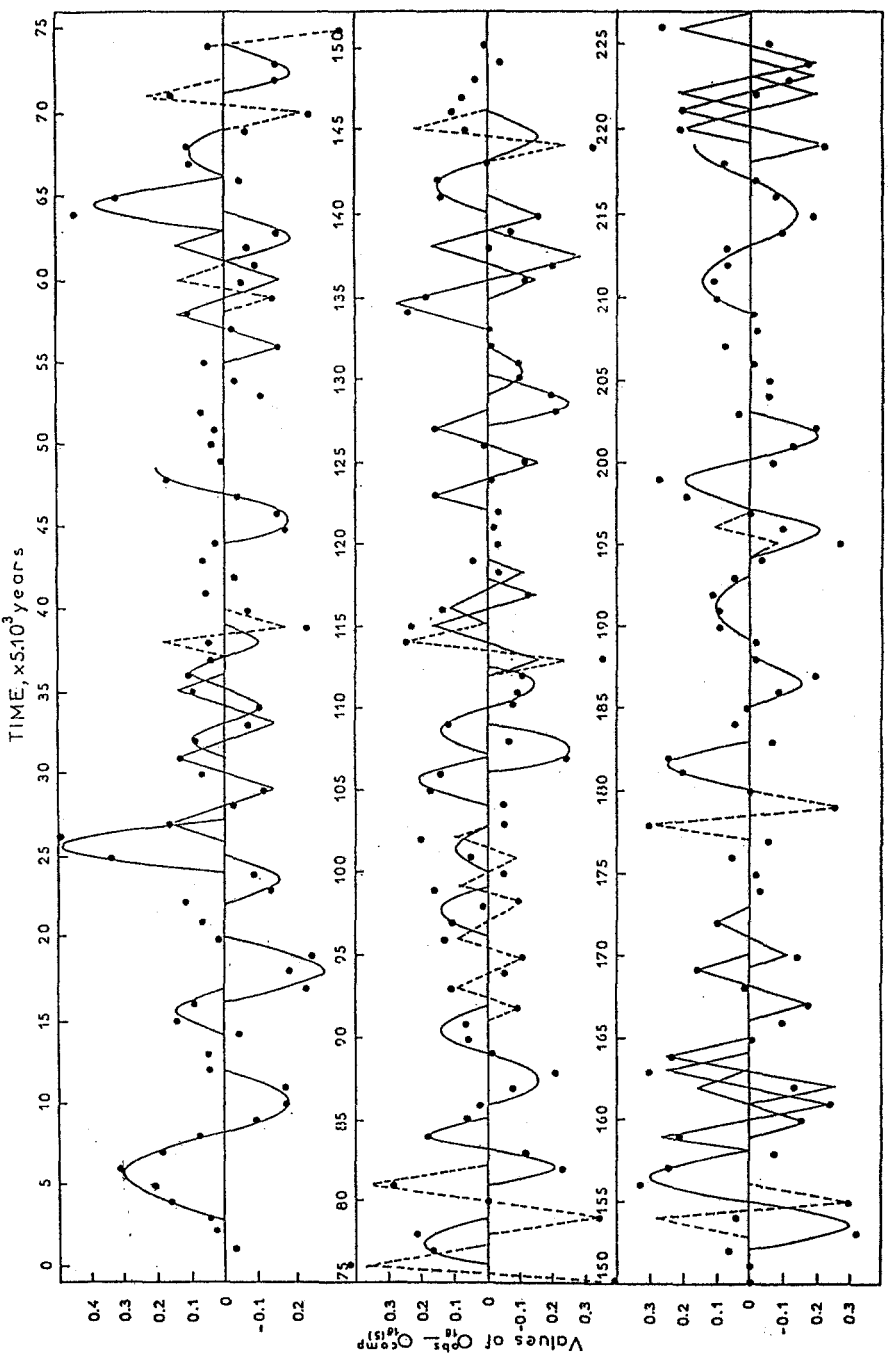

Fig. 10. SA fit of the differences between initial unsmoothed $\delta^{18}O$ values and computed smoothed ones (Equation (3) of the text), with sinusoids having periods 15, 20 and 30 Kyrs.

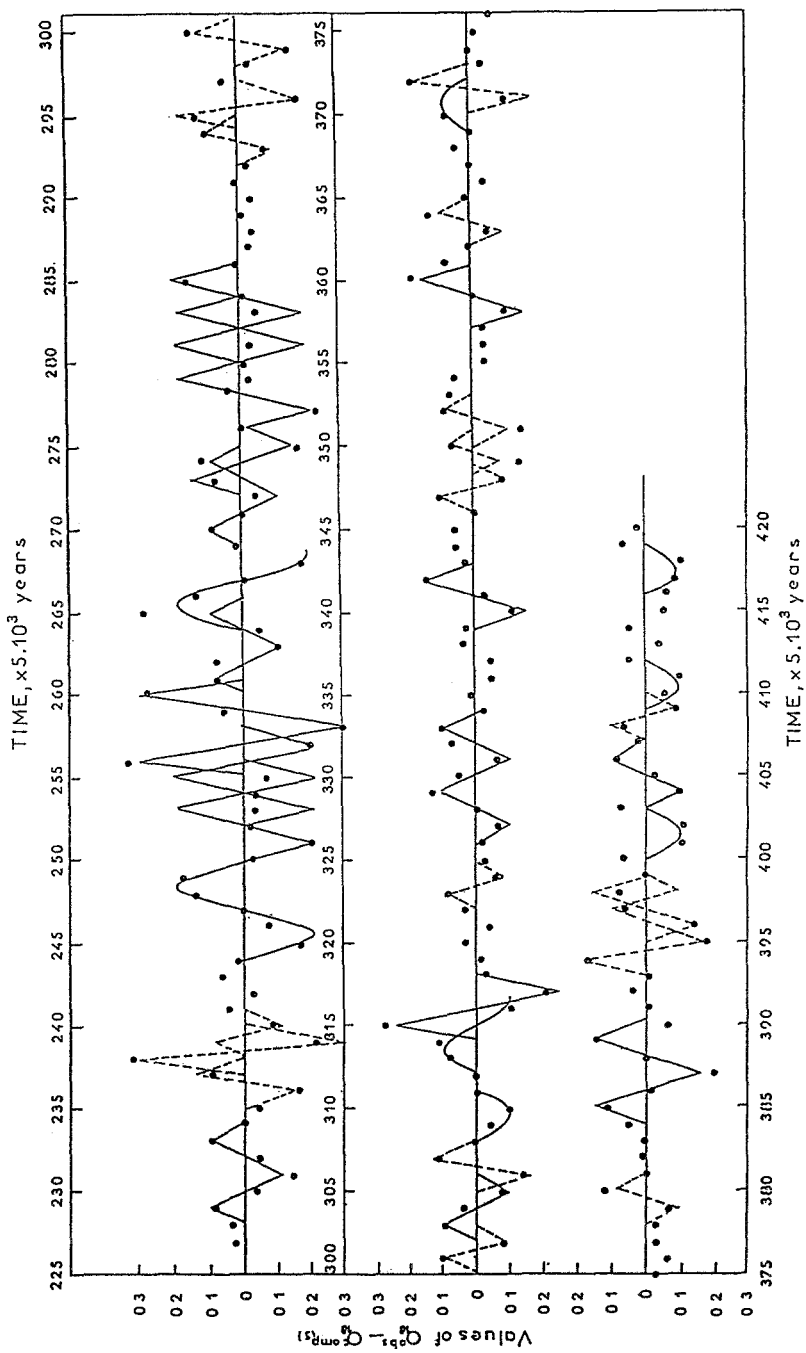

Fig. 10. Continued.

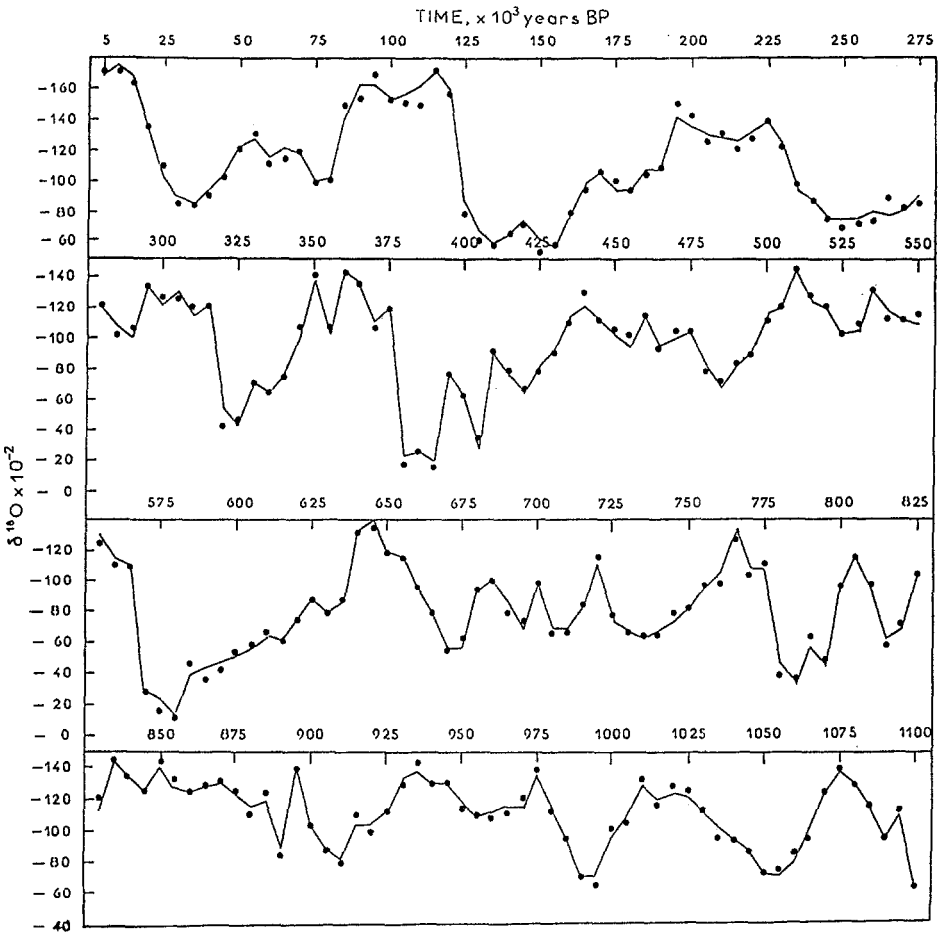

Fig. 11. Final generalised curve of computed values (Equation (4) of the text) (solid line) and original unsmoothed δ^{18}O data (dots).

This equation fits the original data with an accuracy of 96.3%, standard error ± 0.038, $P = 364$ and $DF = 56$.

Discussion

Similar periods have been obtained by other workers analysing other data series (see Table B1 in Berger, 1988).

Previous analyses of the V28-239 and V28-238 pacific ocean cores by MESA has shown that there is a strong tendency for variance to be concentrated at frequencies corresponding to periods of 100, 41, 23 and 19 Kyrs (Berger and Pestiaux, 1984a,b; Berger,1989).

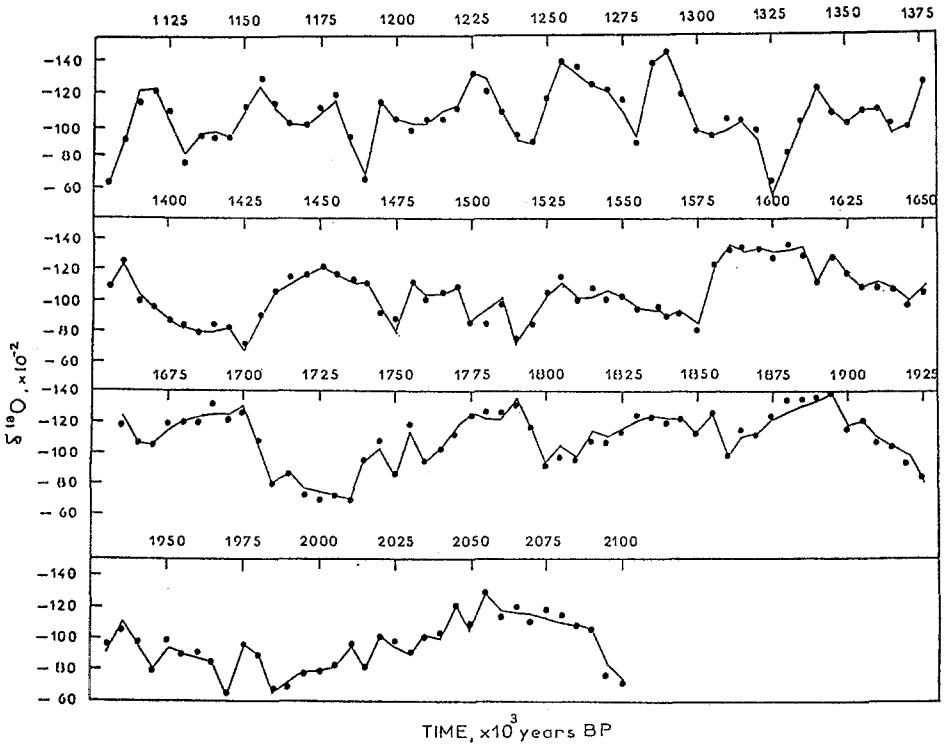

Fig. 11. Continued.

The gradual evolution of δ^{18}8O time-series for V28-239 core has also been demonstrated by Berger and Pestiaux (1984b) using an evolutive procedure of the MESA, particularly for the power change of the 100 Kyr quasi-periodicity. They compared four intervals each 800 Kyrs long which indicated very weak 41 Kyr and 19 Kyr signals in the third interval (0.8–1.6 Myr), equally shared peaks of 23 Kyr and 19 Kyr of precession variance, and for the first (0–0.8 Myr) and fourth (2.4–3.2 Myr) intervals are more or less the same with a moderate 41 Kyr signal, a strong 23 Kyr signal and a moderate to strong 19 Kyr one. The quasi-periodic character of these periods are also found in our Figure 8.

Also, the 100 Kyr cycle, so dominant a feature of the late Pleistocene record does not exhibit a constant amplitude over the past 2–3 Myrs. This periodicity according to Berger and Pestiaux (1984) disappears before 1 million years ago.

Our results indicate constant occurrence of the 100 Kyrs period during the past 2 Myrs.

In our present MESA analysis in conjuction to FFT, the alternative evolution spectra process of subsets, the pseudo-sonogram and the SA method which locates the periods, revealed some new aspects. That is, although our results indicate similar periods to those obtained by Berger and Pestiaux, several secondary ones

TABLE III

α_{1-3} coefficients of periodic terms of Equation (5) and respective time intervals (multiply with 5 Kyrs) where the periods appear.

a_1	T
−0.15	22–25, 86–92, 100–103, 185–188
0.50	24–27
−0.20	43–48, 61–64, 194–203, 244–250
0.40	63–66
0.20	76–79, 104–107, 264–268
0.15	96–99, 107–113, 140–146, 14–17
−0.25	106–109, 127–130
−0.10	129–132, 304–307, 409–412, 416–419
0.25	133–139, 180–183
0.10	145–148, 308–311, 312–316
−0.30	152–158
−0.08	369–372

a_2	T
−0.20	8–12
−0.30	16–20
0.10	189–193
0.15	209–218

a_3	T
0.30	3–8

were recognised and the evolution of the fundamental and secondary astronomical cycles differed.

The periodicities found by the three methods of spectrum analysis, i.e., MESA, FFT and SA, are shown in Table I for comparison. Apart of the dominant 100 Kyrs signal the 41 and 19–23 Kyrs as well as the secondary signals are not strictly stationary, appear as quasi-periods and of variable amplitude, as Figures 8 and 10 show.

All four methods employed here, basically gave similar periods. The exception is for the 500 Kyr, 250 Kyr present in Figure 7, while the 16.2, 17.5, 11.2 and 18 Kyrs quasi-periods (illustrated in Figure 4) were indeterminable by SA due to insuficient data points that form such periods, being also a little below the Nyquist frequency.

The dating of the 21-m long core V28-239 was determined from palaeomagnetic stratigraphy by correlation with adjacent shorter core V28-238 and the ages estimated by linear interpolation in saw-toothed core V28-238 using a rate of 1.7 cm/1000 yr, assisted by characteristics in oxygen-isotope record.

The magnetic stratigraphy indicated an average accumulation rate for V28-239 of 1 cm/1000 yr, thus giving one sample every 5 Kyrs.

However, the somewhat less uniform accumulation rate in V28-239, than in V28-238, may provide less reliable ages within Brunhes magnetic epoch. Certainly, accurate dating is essential if the obtained periodicities are to be meaningfully related to earth's orbital parameters caused climatic changes. Nevertheless, the presence of the main orbital elements from the analysis of present data may well strengthen the suggestion that the newly found periodicities are real, though on the other hand, their exact length depends upon (a) the errors in the age-depth scale of the core, especially true for the lower periodicities, and (b) on the data spacing of 5 Kyrs. Similar analysis on more core data are needful in order to regard these periods as definitive.

For the Figure 7 the two new spectral peaks of 500 and 250 Kyrs may represent sub-harmonics of the fundamental period due to detrending.

The newly employed SA method has a sound result as it actually evaluates the position, phase, and evolution (stationarity) of the periodicities obtained otherwise by the various algorithms in the frequency domain, whereas sophisticated analysis is employed involving significance levels and various other tests are applied to choose the most appropriate analytical methodology.

All periods found are identified to respective climatic cycles driven possibly by astronomical forcing. Of particular notice is the detection of several secondary peaks of the fundamental precession, tilt and eccentricity of the earth's orbit. However, they are of variable occurrence during the past 2 million years. They form a network of periodic terms, where all periodicities found are superimposed on each other. At any rate, by whatever oscillators these periods are caused, non-linear oscillators are characterised by harmonics, sub-harmonics and combination tones of the forcing frequencies and on the other hand by frequency-amplitude dependence of the response.

The newly found (quasi-) periodic terms between 11–18 Kyrs, apart of the age errors as discussed earlier, may be due to these combined effects (Pestiaux *et al.*, 1987) or due to a long term solar activity variation. For the latter, a solar-climatic connection has also been invoked (Rampino *et al.*, 1987; Xanthakis *et al.*, 1992; Sun and Climate, 1980)

The physical reason for the obtained result is not known. This may be the effect of the resultant cumulative insolation curve derived from the summation of the three earth orbital elements whose period differ, while the perturbations of these elements are due to the gravitational effects of the different planets on the earth's orbit and each of them can be expressed as a quasiperiodic function of time (Fairbridge, personal communication to IL).

Fundamental tones based on orbital dynamics of the sun and especially three larger planets, are for example the 6,672 Kyrs and 93,418 Kyrs, while resonances occur mainly at 3rd and 7th tones, thus producing harmonics almost resembling our obtained lower periods.

We seem, here, to deal with a chaotic behaviour of climatic response, emerged from and reinforced by (during long-time intervals, or several decades longer intervals than the period concerned) various stochastic processes.

One, also, has to bear in mind that the geographical latitude of proxy climatic data-series is important in climatic response as insolation is dependent on the relative importance assigned to the three individual orbital components.

Figure 9 predicts, assuming no human interference, a significant temperature drop from present value in the coming 10 Kyrs AP, and major cooling at around 135 Kyrs AP. Until then, alternated cool and warm periods will overlap onto the general mean trend of the time-series.

The diversity among all spectra of different proxy climatic parameters from different locations over the earth is one of the most informative results for understanding how the climatic system responds to insolation forcing.

Also, the application of several methods of spectral analysis to the same time-series enhances the reliability of the obtained periodicities.

The results of our present spectral analysis suggest a network of superimposed periodic oscillators of variable wavelength and amplitude. The implications may be found in the perturbations in the earth's orbital elements and may involve a triggering mechanism for a positive-feedback self-amplifying geoclimatic process. The observed network result may also involve long term (tens of thousands of years) periodic variation of solar radiation (solar constant). For the latter, short-term periodic variations ranging between a few minutes to some thousands of years have been indicated by indirect evidence in solar-terrestrial parameters, i.e., radiocarbon variation in the atmosphere, sunspot numbers, auroral frequency of occurrence, Be-10 in ice varves, solar flares, geomagnetic index, so that a longer periodic variation in solar output is rather compelling (Liritzis, 1990).

We may, thus, encounter common periodicities in both the terrestrial and solar-planetary environment, which interact and form the seemingly chaotic behaviour of O-18 and other proxy climatic data series.

Conclusion

The spectral analysis of $\delta^{18}O$ values from V28-239 pacific ocean deep sea core has revealed a network of periodicities ranging from 10 Kyrs to 1 million years, where the fundamental periods of the earth's orbital elements, i.e., eccentricity, precession and obliquity dominate.

Although the Milankovich astronomical theory to interpret palaeoclimatic variation as inferred from $\delta^{18}O$ changes in foraminifera can be invoked, a simultaneous

common periodic variation in summer insolation due to a periodic solar output variation is an important contempletion, too.

In particular, amongst the methods used (MESA, FOURIER, POWER SPECTRUM) the least squares method of successive approximation of the data by sinusoids determined the existing periods, that is, their length, position and amplitude, and a generalised expression fit to the data was established with a high accuracy at the confidence level of 0.04.

Acknowledgements

We are grateful to Prof. J. C. Duplessy and Prof. A. Berger for their critical evaluation and useful comments and Prof. S. Silverman for loan of his PSA programme. This work is part of a project on "solar activity-palaeoclimates and sediment radioactivity" under the Athens Academy grant no. 200/256.

References

Anderson, N.: 1974, 'On the Calculation of Filter Coefficients for Maximum Entropy Spectral Analysis', *Geophysics* **39**, 69–70.

Akaike, H.: 1969, 'Fitting Autoregressive Models for Prediction', *Ann. Inst. Statis. Math.* **21**, 243–247.

Barton, C. E.: 1983, 'Analysis of Palaeomagnetic Time-Series: Techniques and Applications', *Geophysical Surveys* **5**, 335–368.

Berger, A.: 1988, 'Milankovich Theory and Climate', *Rev. of Geophysics* **26**(4), 624–657.

Berger, A.: 1989, 'Pleictocene Climatic Variability at Astronomical Frequencies', *Quaternary Intern.* **2**, 1–14.

Berger, A. and Pestiaux, P.: 1984a, 'Accuracy and Stability of the Quaternary Terrestrial Insolation', in A. Berger *et al.* (eds), *Milankovich and Climate,* pp. 83–112, D. Reidel Publ. Co, Dordrecht, Netherlands.

Berger, A. and Pestiaux, P.: 1984b, 'Modelling the Astronomical Theory of Palaeoclimates in the Time and Frequency Domain', in A. Ghazi and R. Foutechi (eds), *Current Issues of Climate Research,* pp. 77–96, D. Reidel Publ. Co, Dordrecht, Netherlands.

Burg, J. P.: 1967, 'Maximum Entropy Spectral Analysis', 37th Ann. Int. Meeting Soc. Explor. Geophys. Oklahoma City (see also, PhD thesis, Stanford University, Stanford, Ca.)

Burg, J. P.: 1968, 'A New Analysis for Time-Series Data', *Adv. Study Inst. on Signal Processing.* NATO, Enschede.

Chatfield, C.: 1984, *The Analysis of Time Series. An introduction.* (3rd edition), Chapman and Hall, London.

Emiliani, C.: 1955, 'Pleistocene Temperatures', *J. Geology* **63**(6), 538–578.

Fougere, P. F.: 1977, 'A Solution to the Problem of Spontaneous Line Splitting in Maximum Entropy Power Spectral Analysis', *J. Geophys. Res.* **82**, 1051–1054.

Hays, J. D., Imbrie, J., and Shackleton, N. J.: 1976, 'Variations in the Earth's Orbit: Pacemaker of the Ice Ages', *Science* **194**, 1121–1132.

Jaynes, E. T.: 1982, 'On the Rationale of Maximum Entropy Methods', *Proc. IEEE* **70**(9), 939–952.

Levinson, H.: 1947, 'The Wienner RMS (Root Mean Square) Error Criterion. In Filter Design and Prediction', *J. Math. Phys.* **25**, 261–278.

Liritzis, Y.: 1990, 'Evidence for Periodicities in the Auroral Occurrence Frequency Since 300 AD and their Implications', *PAGEOPH* **133**(2), 201–211.

Rampino, M. R., Sanders, J. E., Newman, W. S. and Konigsson, L. K. (eds): 1987, *Climate: History, Periodicity and Predictability,* Van Nostrand Reinhold Co, New York, pp. 588.

Shackleton, N. J. and Opdyke, N. D.: 1976, 'Oxygen-Isotope and Palaeomagnetic Stratigraphy of Pacific Core V28-239 Late Pliocene to Latest Pleistocene', *Geological Soc. America Memoirs* **145**, 449–464.

Silverman, S. M. and Shapiro, R.: 1983, 'Power Spectrum Analysis of Auroral Occurrence Frequency', *J. Geophys. Res.* **88**(A8), 6310–6316.

Silverman, S. M., Ward, F. W., and Shapiro, R.: 1971, 'Power Spectrum Analysis of the Light Curve of RR Tauri', *Astrophysics and Space* **12**, 319–324.

Smylie, J. E., Clark, G. K. C., and Ulrych, T. J.: 1973, 'Analysis of Irregularities in the Earth's Rotation', in *Methods in Computational Physics,* **13**, 391– 430, Academic Press, N.Y.

Sun and Climate: 1980, *Proceedings of the International Conference on Sun and Climate,* CNES, CNRS and DGRST, Toulouse, France, pp. 471.

Ulrych, T. J. and Bishop, T. N.: 1975, 'Maximum Entropy Spectral Analysis and Autoregressive Decomposition', *Rev. Geophys. Space Phys.* **13**, 183– 200.

Xanthakis, J. and Liritzis, I.: 1989, 'Spectral Analysis of Archaeomagnetic Inclinations for the Last 2000 Years', *Earth, Moon and Planets* **45**, 139– 151.

Xanthakis, J. and Liritzis, I.: 1991, *Geomagnetic Field Variation as Inferred from Archaeomagnetism in Greece and Palaeomagnetism in British Lake Sediments since 7000 B.C.,* Academy of Athens Publication, Vol. 53, pp. 222.

Xanthakis, J., Liritzis, I., and Galloway, R. B.: 1992, 'Periodic Variation in Natural Radioactivity of Lake Bouchet Sediments', *Earth, Moon and Planets* **59**, 191–200.